Proceedings of the ASME 2017 International Design Engineering Technical Conferences & Computers and Information in Engineering Conference
IDETC/CIE 2017
August 6-9, 2017, Cleveland, USA

DETC2017-67649

KINEMATIC CONSTRAINT MAPS, $\mathscr{C}$-SPACE SINGULARITIES AND GENERALISED GRASHOF CONDITIONS

S.Vahid Amirinezhad *
School of Mathematics and Statistics
Victoria University of Wellington
Wellington 6140
New Zealand
Email: vahid.amirinezhad@sms.vuw.ac.nz

Peter Donelan
School of Mathematics and Statistics
Victoria University of Wellington
Wellington 6140
New Zealand
Email: peter.donelan@sms.vuw.ac.nz

ABSTRACT

The kinematics of parallel mechanisms are defined by means of a kinematic constraint map (KCM) that captures the constraints imposed on its links by the joints. The KCM incorporates both pose parameters describing the configuration of every link and the design parameters inherent in the mechanism architecture. This provides a coherent approach to determining $\mathscr{C}$-space singularities and generalised Grashof conditions on the design parameters under which these can occur.

INTRODUCTION

A mechanism singularity is usually interpreted physically as a configuration where an instantaneous change occurs in its *degrees of freedom* (dofs). Mathematically, this is determined by a drop in rank of the Jacobian matrix of its kinematic mapping. While open chain or serial manipulator kinematic singularities are well understood (see, for example, [1–8]), closed chain or parallel manipulator (PM) singularities present a number of challenges and there has been a variety of approaches to their analysis and taxonomy. While the physical and mathematical approaches typically coincide, nevertheless the choice of kinematic mapping can make a difference. One goal of this paper is to present an approach that is, in principle, unified across all types of manipulators and that takes into account the impact on singularities of design parameters in a given architectural family.

A key idea in studying singularities of parallel mechanisms is due to Gosselin and Angeles [9]. Their analysis is based on defining an implicit function combining input and output variables. The resulting Jacobian matrices give rise to two main types of singularity, namely *inverse kinematic*, *forward kinematic*, and the combination of both of these as a special case. The authors note that this third kind of singularity is parameter-dependent within a given architecture.

Zlatanov *et al* [10] extended this approach for parallel mechanism singularities, based directly on an instantaneous velocity equation, so by-passing the implicit function. In addition to input and output velocities, passive-joint velocities were also included, giving rise to a greater variety of singularity classes and providing an explanation for unexpected motion observed in some examples [11].

Park and Kim [12, 13] developed a similar approach based on differential geometry, incorporating a full kinematic map that enabled the identification of *configuration space singularities*, as well as actuator and end-effector singularities. Also known as $\mathscr{C}$-space singularities, these are in some sense more fundamental than the other types since the singularity occurs in the total space of configurations and is independent of choice of input or output variables. A simple case of $\mathscr{C}$-space singularity is well known in the classical mechanism literature and concerns planar 4-bar mechanisms. Here, the occurrence of a $\mathscr{C}$-space singularity is given by a single equation in the design parameters—the link lengths—closely related to the Grashof condition [14]. The idea

*Address all correspondence to this author.

of $\mathscr{C}$-space singularities has been also developed by Zlatanov *et al* [15].

As noted, from the viewpoint of $\mathscr{C}$-space singularities, the motion of all components of a mechanism are relevant. In a parallel mechanism, it is easier to determine the constraints on, rather than the freedoms of, each component. Note that the constraints are not just those arising from closed circuits in the mechanism but that, in fact, every joint imposes constraints on the otherwise free motion of each link (see [16], chapter 4). Piipponen and Tuomela [17] use this idea to arrive at *algebraic* constraint equations. By comparison, our approach is based on differential geometry, enabling the application of the theory of singularities of mappings [18]. In principle, this approach is slightly more comprehensive since it includes helical joints. It also lends itself to singularity descriptions that relate to the Euclidean Lie groups and associated screw systems in the Lie algebras. Moreover, the design parameters play a critical role leading to Grashof-type conditions for $\mathscr{C}$-space singularities. The idea of this type of condition was introduced by Gibson and Newstead [14] and revisited in [19, 20]. The name derives from the associated inequality that Grashof introduced to distinguish between various classes of 4-bar motion [21].

Our approach to parallel mechanism kinematics is novel in several respects. Firstly, we dispense with the mixed use of input and output variables, concentrating instead on the constraints imposed by the joints on the otherwise free motion of the links. This has the additional advantage that closed-loop constraints do not have to be separately represented—they arise automatically from the joint constraint equations. Secondly, by explicitly including design parameters the kinematic analysis can proceed for a whole family of mechanisms. Then, in the search for the most fundamental type of kinematic singularity, namely the $\mathscr{C}$-space singularities that occur in the space of feasible motions independent of the choice of actuated joints or end-effector (platform), the design (Grashof) conditions for singularity can, in principle, be computed from the Jacobian of the constraint map. While we do not explore this in the current paper, the proposed framework will enable computation of the higher level singularity types related to specific choice of input (actuator) and output (end-effector) variables. A further natural extension is to explore transversality conditions that would determine whether, for a given class of mechanisms, a typical (generic) choice of design parameters results in a non-singular $\mathscr{C}$-space.

In the paper, we first introduce the notion of a *kinematic constraint map* (KCM) as the tool for defining the $\mathscr{C}$-space. Underlying aspects of singularity theory relevant to the problem are then described. We present two examples of planar parallel manipulators and determine the conditions for a $\mathscr{C}$-space singularity in terms of the design parameters. The second of these has not previously appeared in the literature. Finally, we present some brief conclusions.

KINEMATIC CONSTRAINT MAPS

The idea of a kinematic constraint map is to provide a consistent description of the kinematic capabilities of a mechanism, independent of the choice of inputs (actuators) and outputs (end-effector). While the choice of these is ultimately critical to the application of a mechanism, the KCM will be able to capture any such choice and from that to determine, among other things, all types of kinematic singularity. The KCM itself, or something analogous to it, is essential for capturing underlying configuration space singularities of the whole mechanism.

The distinction between an approach based on freedoms and one based on constraints is, in a certain way, captured by the two forms of the Chebyshev–Grübler–Kutzbach (CGK) formula determining the global mobility for a generic multibody system:

$$\mu = \sum_{i=1}^{t} \delta_i - n(t-k+1) = n(k-1) - \sum_{i=1}^{t} (n-\delta_i) \qquad (1)$$

where t, δ_i, k are total number of joints, dof of joint i, $i = 1,\ldots,t$, and total number of links respectively, while $n = \dim SE(m)$, $m = 2,3$. The essential point of Eqn. 1 is that although the two formulae are equivalent, they are looking for global mobility μ from different perspectives. The first form expresses mobility in terms of joint freedoms, whereas the second form is in terms of joint constraints, so that the forms are complementary.

Pose parameters

The approach we adopt is first to assign a Euclidean coordinate system to each (rigid) link in a mechanism, denoted a *moving frame*, as well as a *reference frame* in the ambient space, which may be chosen as the coordinate system for a given component, assumed fixed for the purpose of the analysis. The displacement of a given moving frame M with respect to the reference frame R is an element of the Euclidean group $SE(m)$ ($m = 2$ for a planar mechanism and $n = 3$ for spatial). This is called the *absolute displacement* of M [16] and can be described, in terms of a representation of the Euclidean group, by *pose parameters* (PPs).

Note that in the planar case, $\dim SE(2) = 3$, so that three pose parameters are required to represent the displacement of each link. We use on, θ, for rotation about the origin and two translations along axes:

$$(\theta, x, y)^T \in \mathbb{R}^3 \qquad (2)$$

While θ is unique only up to addition of multiples of 2π, nevertheless these parameters are essentially global and non-singular. On the other hand, in the spatial case, $\dim SE(3) = 6$, and six pose parameters are needed: typically three for rotation about

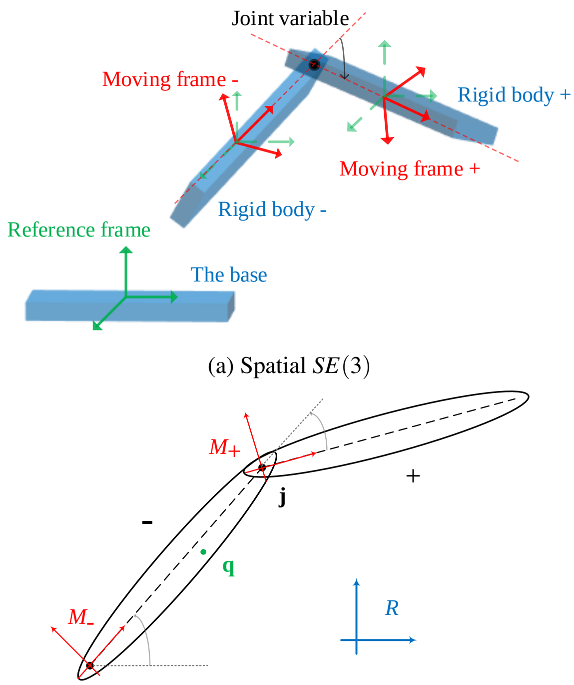

(a) Spatial $SE(3)$

(b) Planar $SE(2)$

FIGURE 1: Two adjacent bodies jointed at a given point $\mathbf{j}$

the origin, for example Euler angles, and 3 for translation along the axes:

$$(\theta,\phi,\psi,x,y,z)^T \in \mathbb{R}^6 \tag{3}$$

In this case, since the rotation subgroup is double-covered by the 3-sphere S^3, there is not a non-singular global choice of angular parameters. An alternative is to use Euler parameters or quaternions as homogeneous coordinates. In each case, we have effectively used the semi-direct product decomposition of the Euclidean group, $SE(m) \cong SO(m) \times \mathbb{R}^m$. In this decomposition, we typically denote an element of the Euclidean group by a pair $(A,\mathbf{a})$.

If a point in a given link with absolute displacement $(A,\mathbf{a})$ has coordinates $\mathbf{q}$ in its moving frame, then its coordinates in the reference frame are given by:

$$\mathbf{Q} = A\mathbf{q} + \mathbf{a}. \tag{4}$$

Joint constraint equations

A displacement of a link with respect to an adjacent link, connected to it by a joint, is called a *relative displacement*. The goal is to emulate [17] and establish constraint equations representing the joint. These then determine the constraints on relative displacements. We establish how to do this in the simplest case of a planar revolute joint. In this case the constraint is that the absolute coordinates [16] of the joint's coordinates with respect to the two moving frames coincide in the reference frame. This is illustrated in in Fig. 1.

In the notation, $-$ and $+$ stand for, nominally, the preceding and following bodies. Hence, the joint $\mathbf{j}$, in Fig. 1(b), constrains their relative motion. If the joint has coordinates $\mathbf{j}_\pm$ in the frames $M_\pm$, and the links have pose parameters determined by $(A_\pm,\mathbf{a}_\pm)$, then, by Eqn. 4, in the reference frame R:

$$\mathbf{J}_\pm = A_\pm \mathbf{j}_\pm + \mathbf{a}_\pm \tag{5}$$

are the joint's absolute coordinates. This entails the vector equation:

$$\mathbf{J}_+ = \mathbf{J}_- \Longrightarrow (A_+\mathbf{j}_+ + \mathbf{a}_+) - (A_-\mathbf{j}_- + \mathbf{a}_-) = \mathbf{0} \in \mathbb{R}^2 \tag{6}$$

in terms of the two sets of pose parameters. The revolute joint translates into two scalar constraints on the pose parameters. Note also that $\mathbf{j}_\pm$ will usually be dependent on the mechanism's design parameters, such as link lengths, hence the equations embody these parameters.

By way of comparison, a spatial revolute joint can be described by the coincidence of a line and a point on that line in each adjacent link. This gives rise to five scalar constraint equations. More simply, a spherical or ball joint is analogous to a planar revolute joint, requiring coincidence of two points, thus three scalar equations.

As in Eqn. 1, a given mechanism consists of k rigid links connected to each other by t kinematic pairs. Each joint imposes constraints on the whole structure in the space of $k \times n$ pose parameters ($n = \dim SE(m)$). We now define the **kinematic constraint map** for a mechanism to be the map f determined by the expressions in the joint constraint equations, Eqn. 6, across all joints. In other words, the map is:

$$f : \mathscr{M} \longrightarrow \mathbb{R}^r \tag{7}$$

with domain $\mathscr{M} = [SE(m)]^k$, and $r = \sum_{i=1}^{t}(n-\delta_i)$ as in Eqn. 1, the total number of (scalar) constraint equations. We regard, at least locally, $\mathscr{M}$ to be parametrised by $p = k \times n$ pose parameters. Note that if one component of the mechanism is treated as fixed then k can be replaced by $k-1$ in the definition of $\mathscr{M}$. In this form, the CGK becomes an expression of the dimension of the **configuration space**:

$$\mathscr{C} := f^{-1}(\mathbf{0}_r) \subset \mathscr{M} \tag{8}$$

under the assumption that $\mathbf{0}_r$ is a regular value of f, by the Pre-Image Theorem (see, for example, Theorem 2.8 in [18]). In general, $\mathscr{C}$ will be an analytic variety but, without the regularity condition, may have singularities.

By contrast, approaches like that of Gosselin and Angeles [9] effectively represent the KCM, for a mechanism in dimension $m = 2,3$, as:

$$f : \mathscr{J} \times \mathscr{E} \longrightarrow \mathbb{R}^e \tag{9}$$

where $\mathscr{J} \subseteq \mathbb{R}^d$, $d = \sum_{i=1}^{t_a} \delta_i$, with the first t_a joints assumed actuated or inputs, $\mathscr{E} = SE(m)$ represents the outputs or pose parameters of the end-effector/platform and $e = m \times \ell$, where ℓ is the number of independent cycles in the mechanism's architecture. The extensions of Zlatanov *et al* [10] and Park and Kim [13] extend $\mathscr{J}$ to admit passive joints but still retain the mix of domain coordinates.

$\mathscr{C}$-SPACE SINGULARITIES

As noted in the previous section, the configuration space $\mathscr{C}$ may have singularities. The matrix of first-order partial derivatives—the Jacobian matrix—of the KCM in Eqn. 7 with respect to local parametrisations of the Euclidean groups must be computed to determine singularities. These are points where the Jacobian of KCM is rank deficient, the singular set of f:

$$\Sigma f = \{\mathbf{u}_s \in \mathscr{M} \mid \mathrm{rank} Jf < r\} \tag{10}$$

Then, the $\mathscr{C}$-space *singularity set* is the set of points:

$$\Sigma_{\mathscr{C}} := \Sigma f \cap \mathscr{C} \tag{11}$$

so, in addition, the joint constraint equations are satisfied. Both conditions in Eqns. 10 and 11 are required to conclude that there are $\mathscr{C}$-space singularities within a family of mechanisms. Note that for some over-constrained mechanisms the Σf may not be transverse to the $\mathscr{C}$-space so that the whole of $\mathscr{C}$ may be singular in this sense.

Mathematically, the set of critical (non-regular) values of any smooth function, such as the KCM $f : \mathscr{M} \longrightarrow \mathbb{R}^r$ form a set of measure zero (this is Sard's Theorem [18], p.34). In effect almost every point in $\mathbb{R}^r$ is regular, so that we would expect a given $\mathscr{C}$-space to have no singularities. However this will likely depend on the design parameters. Suppose the vector of possible design parameters form a space $\mathscr{D} \subseteq \mathbb{R}^s$ where s is the total number of design parameters. Then we can think of the *extended* KCM as a parametrised family of functions:

$$F : \mathscr{M} \times \mathscr{D} \to \mathbb{R}^r \tag{12}$$

This is the setting for the parametrised Transversality Theorem [18], Lemma 4.6. In effect, for almost all choices of design parameters, $\mathbf{d} \in \mathscr{D}$, the associated KCM will have no singularities. The question arises, can we determine conditions on the design parameters for the presence of $\mathscr{C}$-space singularities?

Singularity set

The Jacobian of KCM is a rectangular $r \times p$ matrix:

$$Jf = \left[\frac{\partial f_j}{\partial u_i}\right] \tag{13}$$

where $i = 1, \ldots, p = nk$ (or $p = n(k-1)$ if one link is assumed fixed) indexing the pose parameters u_i, and $j = 1, \ldots, r$ indexing the joint constraint equations. Note that unless every joint is locked (immobile), $p > r$. At a regular point $\mathbf{u}_r \in \mathscr{M}$, this matrix is full rank and its cokernel (the quotient of the range by the image) is trivial or dimension zero. At a singular or critical point $\mathbf{u}_s \in \mathscr{M}$, this dimension will be a positive quantity κ called the *corank* or rank deficiency; κ provides a useful measure of how bad a singularity is and we can partition the singularity set Σf into subsets $\Sigma^\kappa f$ for $\kappa = 1, \ldots, \mu = p - r$, the global mobility μ. This, in turn, induces a partition of the $\mathscr{C}$-space singularities by taking their intersections:

$$\Sigma_{\mathscr{C}}^\kappa := \Sigma^\kappa f \cap \mathscr{C} \tag{14}$$

For the purposes of this paper we do no more than determine conditions under which $\Sigma_{\mathscr{C}}$ in Eqn. 11 is non-empty. However, it is useful to consider the number of conditions required for singularities of a given corank.

One can prove that in the set of all $r \times p$ matrices, where it is assumed that $p > r$, the subset Σ^κ of matrices of corank κ is a submanifold and its codimension is given by [18]:

$$\mathrm{codim}(\Sigma^\kappa) := \kappa(p - r + \kappa). \tag{15}$$

Since corank is lower semi-continuous, it is clear that, for each κ, $\Sigma^{\kappa+1}$ lies in the closure of Σ^κ and is of higher codimension. Provided that the KCM satisfies the technical condition, analogous to regularity, that its 1-jet extension (effectively the map that returns the Jacobian matrix at each point of $\mathscr{M}$) is transverse to the submanifolds Σ^κ, then the singularity sets $\Sigma^\kappa f \subset \mathscr{M}$ are submanifolds of the same codimension. Moreover, we would expect that:

$$\begin{aligned}\dim(\Sigma_{\mathscr{C}}^\kappa) &= p - (\mathrm{codim}(\mathscr{C}) + \mathrm{codim}(\Sigma^\kappa)) \\ &= p - (r + \kappa(p - r + \kappa)) \\ &= (1-\kappa)(p-r) - \kappa^2\end{aligned} \tag{16}$$

This quantity is negative for all $\kappa \geq 1$ so that we expect the $\mathscr{C}$-space to be non-singular. However if we also consider the space $\mathscr{D}$ of design parameters, then the first term p in Eqn. 16 is replaced by $p+s$. In particular, for $\kappa = 1$, we obtain $s-1$ for the dimension and this will, generically, be a non-empty set. In fact, it indicates there should be one (Grashof-type) condition on the space of design parameters.

It is important to note that a number of technical conditions are required to ensure this analysis is valid. However, for any particular example we can proceed as follows in order to determine the conditions for singularity. First we compute the Jacobian of the KCM in terms of both pose and design parameters. Determine conditions for the corank to be positive, again in terms of both sets of parameters. Finally, substitute any solutions into the joint constraint equations. This substitution determines the conditions for the $\mathscr{C}$-space to have singularities.

GENERALIZED GRASHOF CONDITIONS

In this section, we develop the kinematic analysis via the KCM for two planar mechanisms. The planar 4R linkage is much studied in the classical literature and the condition for $\mathscr{C}$-space singularity in terms of the link lengths $l_i, i = 0,1,2,3$ is well known to be $l_0 \pm l_1 \pm l_2 \pm l_3 = 0$. We term this, by a slight abuse of its standard meaning, the *Grashof condition* for the mechanism. We note that, for example in [10], the kinematic analysis for the mechanism is carried out using the input/output variable technique. The KCM approach is presented here by way of comparison. While we do not have the space in this paper to show how previous approaches can all be viewed as special cases of this fully general method, we note that any choice of input and output variables can be captured by appropriate choice of columns of the Jacobian. On the other hand, in [10], the method does not permit the coupler bar as output since its motion is not captured by a unique choice of variables. Moreover, the KCM method provides a global rather than local analysis of singularity.

The second example, also well studied is the planar 3RRR manipulator. Once again we make no assumptions about input and output variables but obtain a generalised Grashof condition that has not appeared previously.

Planar 4-bar linkage

This linkage is made up of 4 rigid links ($k = 4$) as in Fig. 2. It has four design parameters $l_i, i = 0,1,2,3$ which are the lengths of its rigid links. Note that l_0 is the base which we will regard as fixed. Each other link has three pose parameters $(\theta_i, x_i, y_i)^T; i = 1,2,3$.

Define a reference frame R and moving frames M_i, $i = 1,2,3$ as in Fig. 2. The moving coordinates of each joint $\mathbf{j}_i \in \mathbb{R}^2, i = 1,2,3,4$ with respect to the frames of links it connects are as follows (where the superscript identifies the frame):

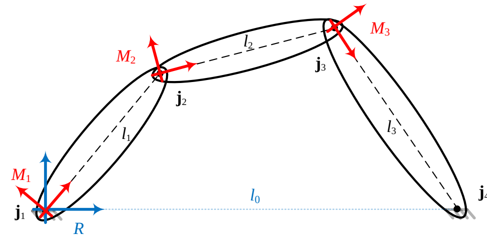

FIGURE 2: 4-bar linkage with associated frames and design parameters

$$
\begin{aligned}
\mathbf{j}_1^R &= (0,0)^T \ , \ \mathbf{j}_1^1 = (0,0)^T \\
\mathbf{j}_2^1 &= (l_1,0)^T \ , \ \mathbf{j}_2^2 = (0,0)^T \\
\mathbf{j}_3^2 &= (l_2,0)^T \ , \ \mathbf{j}_3^3 = (0,0)^T \\
\mathbf{j}_4^3 &= (l_3,0)^T \ , \mathbf{j}_4^R = (l_0,0)^T
\end{aligned} \tag{17}
$$

We now obtain the reference frame coordinates of the joints in both forms, by using Eqn. 4:

$$
\begin{aligned}
\mathbf{J}_1^R &= A_R \mathbf{j}_1^R + \mathbf{a}_R \ , \ \mathbf{J}_1^1 = A_1 \mathbf{j}_1^1 + \mathbf{a}_1 \\
\mathbf{J}_2^1 &= A_1 \mathbf{j}_2^1 + \mathbf{a}_1 \ , \ \mathbf{J}_2^2 = A_2 \mathbf{j}_2^2 + \mathbf{a}_2 \\
\mathbf{J}_3^2 &= A_2 \mathbf{j}_3^2 + \mathbf{a}_2 \ , \ \mathbf{J}_3^3 = A_3 \mathbf{j}_3^3 + \mathbf{a}_3 \\
\mathbf{J}_4^3 &= A_3 \mathbf{j}_4^3 + \mathbf{a}_3 \ , \mathbf{J}_4^R = A_R \mathbf{j}_4^R + \mathbf{a}_R
\end{aligned} \tag{18}
$$

Equation 6, can now be applied to each joint in turn:

$$
\begin{aligned}
&\text{joint 1 constraining } l_1 \text{ to the } l_0\text{: } \mathbf{J}_1^R - \mathbf{J}_1^1 = 0 \Longrightarrow \mathbf{a}_1 - \mathbf{j}_1^R \\
&\text{joint 2 constraining } l_2 \text{ to } l_1\text{:} \quad \mathbf{J}_2^1 - \mathbf{J}_2^2 = 0 \Longrightarrow A_1 \mathbf{j}_2^1 + \mathbf{a}_1 - \mathbf{a}_2 \\
&\text{joint 3 constraining } l_3 \text{ to } l_2\text{:} \quad \mathbf{J}_3^2 - \mathbf{J}_3^3 = 0 \Longrightarrow A_2 \mathbf{j}_3^2 + \mathbf{a}_2 - \mathbf{a}_3 \\
&\text{joint 4 constraining the } l_0 \text{ to } l_3\text{: } \mathbf{J}_4^3 - \mathbf{J}_4^R = 0 \Longrightarrow A_3 \mathbf{j}_4^3 + \mathbf{a}_3 - \mathbf{j}_4^R
\end{aligned} \tag{19}
$$

With a choice of moving frames and reference frame as illustrated in Fig. 2, the four revolute joints result in 8 scalar joint constraint equations as in Eqn. 6. The resulting KCM $f : SE(2)^3 \longrightarrow \mathbb{R}^8$ can then be written in terms of the parametrisation in Eqn. 2 as:

$$f : (\theta_1, x_1, y_1, \theta_2, x_2, y_2, \theta_3, x_3, y_3) \longmapsto \begin{bmatrix} x_1 \\ y_1 \\ l_1c_1 + x_1 - x_2 \\ l_1s_1 + y_1 - y_2 \\ l_2c_2 + x_2 - x_3 \\ l_2s_2 + y_2 - y_3 \\ l_3c_3 + x_3 - l_0 \\ l_3s_3 + y_3 \end{bmatrix} \tag{20}$$

where $c_i = \cos\theta_i$ and $s_i = \sin\theta_i$, $i = 1,2,3$. The null-set $f^{-1}(\mathbf{0})$ defines the $\mathscr{C}$-space for the 4-bar linkage. Taking derivatives of Eqn. 20 yields an 8×9 Jacobian matrix which, following row operations and deletions of rows and columns with leading 1s, can be reduced to a 2×3 matrix that is sufficient to determine rank deficiency:

$$\begin{bmatrix} -l_1s_1 & -l_2s_2 & -l_3s_3 \\ l_1c_1 & l_2c_2 & l_3c_3 \end{bmatrix} \tag{21}$$

In this case, the translational pose parameters can be eliminated so that the singularity condition depends only on the "free" rotational parameter for each joint and the design parameters. Indeed that is also possible in the joint constraint equations themselves. The singular set Σf is defined by all maximal (2×2) minors vanishing simultaneously and hence:

$$\theta_i = \theta_j + \eta_{ij}\pi : i,j = 1,2,3 \quad ; \quad \eta_{ij} \in \mathbb{Z} \tag{22}$$

Geometrically, the three mobile links must be parallel. It also follows that $c\theta_j = \pm c\theta_i$ and $s\theta_j = \pm s\theta_i$ for each pair i,j. Substituting Eqn. 22 in Eqn. 20 and setting $f = \mathbf{0}$ results in $(l_1 \pm l_2 \pm l_3)s\theta_1 = 0$ and $(l_1 \pm l_2 \pm l_3)c\theta_1 = l_0$. Assuming $l_0 > 0$, we obtain $\theta_1 = 0$ or π and hence:

$$l_0 \pm l_1 \pm l_2 \pm l_3 = 0. \tag{23}$$

Only when this Grashof-type condition holds, there is a $\mathscr{C}$-space singularity and geometrically it corresponds to the 4-bar reaching a flat configuration as illustrated in Fig. 3. As noted previously, the condition in Eqn. 23 is well known. We include its derivation as a case study to validate the approach.

3RRR planar parallel manipulator

The 3RRR planar PM is illustrated in Fig. 4 which shows a choice of moving and reference frames together with design parameters. The mechanism consists of $k = 8$ rigid bodies where

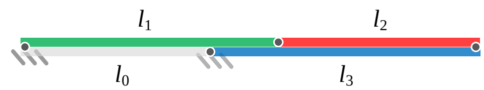

FIGURE 3: 4-bar configuration corresponding to a $\mathscr{C}$-space singularity

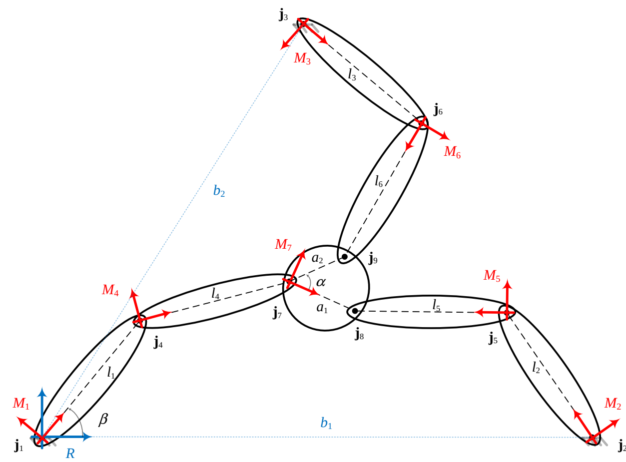

FIGURE 4: Multi-body system of the 3RRR planar manipulator

we regard the ambient space as the fixed base. Therefore we require 21 pose parameters and there are 12 design parameters:

$$\begin{aligned} &\text{design parameters of the links:} && l_i, i = 1,\ldots,6 \\ &\text{design parametrs of the platform:} && a_1, a_2, \alpha \\ &\text{design parameters of the base:} && b_1, b_2, \beta \end{aligned} \tag{24}$$

With the chosen reference and moving frames, the local coordinates of each of the 9 revolute joints in 'preceding' and 'following' frames can be identified in the same way that is for the 4-bar:

$$\begin{aligned} &\mathbf{j}_i^+ = \begin{bmatrix} 0 \\ 0 \end{bmatrix}; i = 1,\ldots,7 \\ &\mathbf{j}_8^7 = \begin{bmatrix} a_1 \\ 0 \end{bmatrix} \quad \mathbf{j}_9^7 = \begin{bmatrix} a_2c_\alpha \\ a_2s_\alpha \end{bmatrix} \\ &\mathbf{j}_i^- = \begin{bmatrix} l_{i-3} \\ 0 \end{bmatrix}; i = 4,\ldots,9 \\ &\mathbf{j}_1^R = \begin{bmatrix} 0 \\ 0 \end{bmatrix} \quad \mathbf{j}_2^R = \begin{bmatrix} b_1 \\ 0 \end{bmatrix} \quad \mathbf{j}_3^R = \begin{bmatrix} b_2c_\beta \\ b_2s_\beta \end{bmatrix} \end{aligned} \tag{25}$$

To find the global coordinates of each point in Eqn. 25, we can follow the same procedure as in Eqn. 18 by means of Eqn. 4.

Since all kinematic pairs in Fig. 4 are planar revolute, all joint constraints associated to this planar PM can be found by using Eqn. 6. Each of the 9 revolute joints imposes a pair of constraint equations, so the KCM has the form $f : SE(2)^7 \to \mathbb{R}^{18}$ given by:

$$(\theta_i, x_i, y_i)_{i=1}^{7} \longmapsto \begin{bmatrix} x_1 \\ y_1 \\ -b_1 + x_2 \\ y_2 \\ -b_2 c_\beta + x_3 \\ -b_2 s_\beta + y_3 \\ -l_1 s_1 - x_1 + x_4 \\ -l_1 s_1 - y_1 + y_4 \\ -l_2 c_2 - x_2 + x_5 \\ -l_2 s_2 - y_2 + y_5 \\ -l_3 c_3 - x_3 + x_6 \\ -l_3 s_3 - y_3 + y_6 \\ -l_4 c_4 - x_4 + x_7 \\ -l_4 s_4 - y_4 + y_7 \\ a_1 c_7 - l_5 c_5 - x_5 + x_7 \\ a_1 s_7 - l_5 s_5 - y_5 + y_7 \\ a_2 c_{\alpha 7} - l_6 c_6 - x_6 + x_7 \\ a_2 s_{\alpha 7} - l_6 s_6 - y_6 + y_7 \end{bmatrix} \tag{26}$$

The $\mathscr{C}$-space is defined as $\mathscr{C} := f^{-1}(\mathbf{0})$.

The associated Jacobian matrix is an 18×21. As for the 4-bar, the problem of determining rank deficiency can be reduced to considering the following 6×9 matrix:

$$\begin{bmatrix} 1 & 0 & l_1 s_1 & 0 & 0 & l_1 s_4 & 0 & 0 & 0 \\ 0 & 1 & -l_1 c_1 & 0 & 0 & -l_1 c_4 & 0 & 0 & 0 \\ 1 & 0 & 0 & l_2 s_2 & 0 & 0 & l_5 s_5 & 0 & -a_1 s_7 \\ 0 & 1 & 0 & -l_2 c_2 & 0 & 0 & -l_5 c_5 & 0 & a_1 c_7 \\ 1 & 0 & 0 & 0 & l_3 s_3 & 0 & 0 & l_6 s_6 & -a_2 s_{\alpha 7} \\ 0 & 1 & 0 & 0 & -l_3 c_3 & 0 & 0 & -l_6 c_6 & a_2 c_{\alpha 7} \end{bmatrix} \tag{27}$$

where $c_i = \cos\theta_i$, $i = 1, \ldots, 7$, $c_{\alpha 7} = \cos(\alpha + \theta_7)$ and similarly for sines.

To determine Σf we must solve simultaneously the vanishing of determinants of the 84 (6×6) minors (see Appendix A for some of the details). From Eqn. 15, the corank 1 singularities are expected to have codimension 4, in other words 4 conditions or equations are required to determine singularity. Many of the minor determinants factorise and it becomes relatively straightforward to deduce that there are three possible conditions that correspond to collinearity of three closed 6R chains within the mechanism and one further condition corresponding to collinearity of the six leg links.

$$\theta_i = \theta_j + \eta_{ij}\pi \qquad i, j \in \{1,2,4,5,7\} \tag{28a}$$
$$\theta_i = \theta_j + \delta_{j7}\alpha + \eta_{ij}\pi \qquad i, j \in \{1,3,4,6,7\} \tag{28b}$$
$$\theta_i = \theta_j + \delta_{j7}(\pi - \gamma) + \eta_{ij}\pi \qquad i, j \in \{2,3,5,6,7\} \tag{28c}$$
$$\theta_i = \theta_j + \eta_{ij}\pi \qquad i, j \in \{1,2,3,4,5,6\} \tag{28d}$$

Here $\eta_{ij} \in \mathbb{Z}$ and δ_{j7} is zero unless $j = 7$ when it is 1; the corresponding angles, $\theta_7 + \alpha$ and $\theta_7 + \pi - \gamma$ in Eqns. 28b, 28c are the angles the platform makes with the corresponding line joining the base anchor points in the closed chain. Note that the first three conditions are expressed by 4 equations but the fourth requires 5 equations and therefore imposes additional conditions on design parameters.

Substituting the singularity conditions into the KCM and setting equal to zero determines the conditions on design parameters—generalized Grashof conditions—necessary for a $\mathscr{C}$-space singularity. Equation 28a fairly easily leads to:

$$b_1 \pm a_1 \pm l_1 \pm l_4 \pm l_2 \pm l_5 = 0. \tag{29}$$

Geometrically, the chain folds into a flattened hexagon. This is illustrated in Fig. 5a. It is possible to make similar deductions for the following two singularity sets in Eqns. 28b and 28c providing two different Grashof-type conditions in the form of Eqn. 29 for the other chains. However, an argument by symmetry, via an appropriate relabelling of the base and platform design parameters leads more simply to the same conclusion for the other closed chains as it is shown in Figs 5b and 5c.

The diagram also shows that in a singular configuration there are potentially four combinations (see Appendix B for more details) of pose parameters for the remaining 2-link leg though in practice not all of these may be feasible.

The final singularity condition, Eqn. 28d, when combined with the joint constraint equations, can be shown to give following pair of generalised Grashof conditions:

$$\begin{aligned} b_1^2\vartheta^2 + b_2^2\zeta^2 &- 2b_1 b_2 \zeta\vartheta\cos\beta \\ &= a_1^2\vartheta^2 + a_2^2\zeta^2 - 2a_1 a_2 \zeta\vartheta\cos\alpha, \end{aligned} \tag{30}$$
$$\begin{aligned} a_1^2 b_1^2 + a_2^2 b_2^2 &- 2a_1 a_2 b_1 b_2 \cos(\beta - \alpha) \\ &= a_1^2\vartheta^2 + a_2^2\zeta^2 - 2a_1 a_2 \zeta\vartheta\cos\alpha. \end{aligned} \tag{31}$$

where $\zeta = \pm l_1 \pm l_4 \pm l_2 \pm l_5$ and $\vartheta = \pm l_1 \pm l_4 \pm l_3 \pm l_6$. These special cases are illustrated in Fig. 6 (see Appendix B for a summary of this analysis).

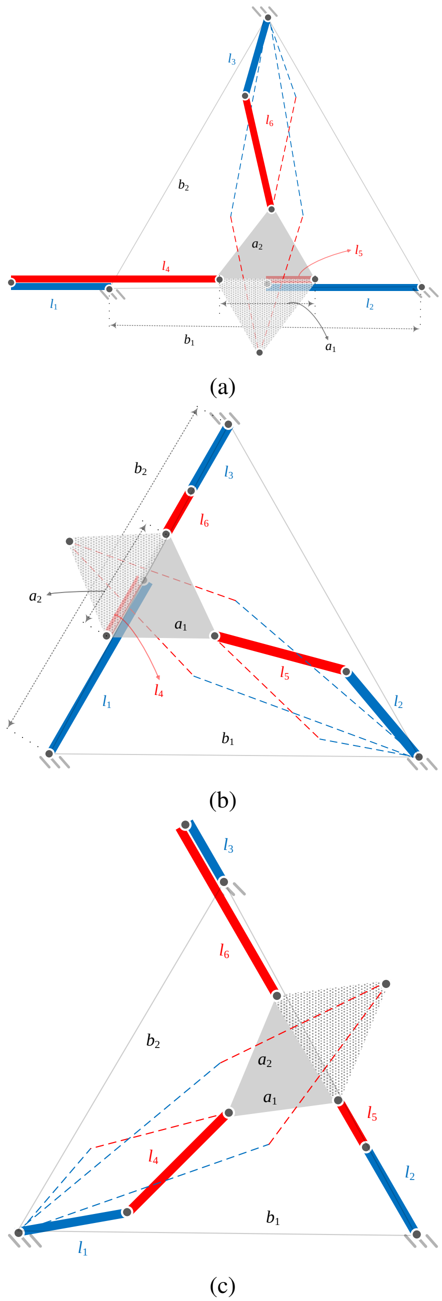

FIGURE 5: Singular $\mathscr{C}$-space configurations for 3RRR planar mechanism

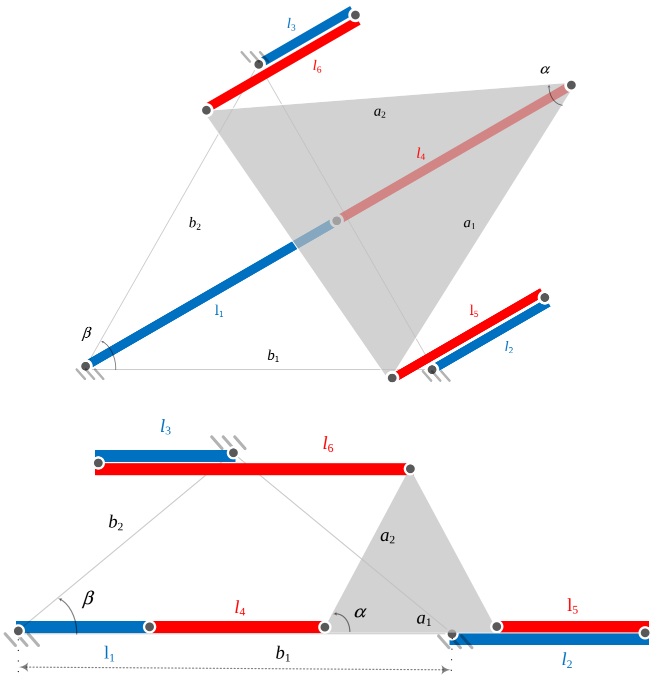

FIGURE 6: Special singular $\mathscr{C}$-space configurations for 3RRR

CONCLUSION

We introduced the idea of kinematic constraint map as a consistent approach to describing the kinematics of mechanisms, whether serial or parallel. A key aim was to avoid the potential confusion in prioritising some joints in terms of their freedoms while leaving others to be subject only to constraints. In our approach, all joints are treated as imposing constraints only. This enables a coherent approach to determining $\mathscr{C}$-space singularities and we have shown, by means of two examples, that their occurrence can be characterised by generalised Grashof conditions. The KCM Jacobian contains submatrices that would enable conditions for direct and inverse kinematic singularities to be determined and subject to choices of actuated joints and output and this will be the subject of further research.

Another advantage of proposed approach based on pose parameters and constraints, is that although one might attain a similar analysis by writing the kinematic map in terms of joint variables, we will be able to deduce the screw system (or its planar equivalent) of each of the components of a given mechanism in any configuration directly from the kernel of the KCM Jacobian, by applying right or left pullback in the corresponding Lie group. This will be the subject of further research.

ACKNOWLEDGMENT

The authors would like to thank Professor Andreas Müller for helpful discussions and insights regarding the methods developed in this paper.

REFERENCES

[1] Sugimoto, K., Duffy, J., and Hunt, K. H., 1982. "Special configurations of spatial mechanisms and robot arms". *Mechanism and Machine Theory,* ***17***(2), pp. 119–132.

[2] Litvin, F. L., Yi, Z., Parenti-Castelli, V., and Innocenti, C., 1986. "Singularities, configurations, and displacement functions for manipulators". *International Journal of Robotics Research,* ***5***(2), pp. 52–65.

[3] Stanisic, M., and Engelberth, J., 1988. "A geometric description of manipulator singularities in terms of singular surfaces". In Proceedings 1st International Workshop on Advances in Robot Kinematics, pp. 132–141.

[4] Pai, D. K., and Leu, M. C., 1989. "Generic singularities of robot manipulators". In Proceedings 1989 IEEE International Conference on Robotics and Automation, IEEE, pp. 738–744.

[5] Burdick, J. W., 1995. "A recursive method for finding revolute-jointed manipulator singularities". *Journal of Mechanical Design,* ***117***(1), pp. 55–63.

[6] Karger, A., 1996. "Singularity analysis of serial robot-manipulators". *Journal of Mechanical Design,* ***118***(4), pp. 520–525.

[7] Tchoń, K., and Muszynski, R., 1998. "Singular inverse kinematic problem for robotic manipulators: a normal form approach". *IEEE Transactions on Robotics and Automation,* ***14***(1), pp. 93–104.

[8] Muller, A., 2012. "On the manifold property of the set of singularities of kinematic mappings: Modeling, classification, and genericity". *Journal of Mechanisms and Robotics,* ***3***(1), 011006.

[9] Gosselin, C., and Angeles, J., 1990. "Singularity analysis of closed-loop kinematic chains". *IEEE Journal of Robotics and Automation,* ***6***(3), pp. 281–290.

[10] Zlatanov, D., Fenton, R. G., and Benhabib, B., 1998. "Identification and classification of the singular configurations of mechanisms". *Mechanism and Machine Theory,* ***33***(6), pp. 743–760.

[11] Di Gregorio, R., 2003. "Kinematics of the 3-UPU wrist". *Mechanism and Machine Theory,* ***38***(3), pp. 253–263.

[12] Park, F. C., and Kim, J. W., 1998. "Manipulability of closed kinematic chains". *Journal of Mechanical Design,* ***120***(4), pp. 542–548.

[13] Park, F. C., and Kim, J. W., 1999. "Singularity analysis of closed kinematic chains". *Journal of Mechanical Design,* ***121***(1), pp. 32–38.

[14] Gibson, C. G., and Newstead, P. E., 1986. "On the geometry of the planar 4-bar mechanism". *Acta Applicandae Mathematicae,* ***7***(2), pp. 113–135.

[15] Zlatanov, D., Bonev, I. A., and Gosselin, C. M., 2002. "Constraint Singularities as C-Space Singularities". In Advances in Robot Kinematics, J. Lenarčič and F. Thomas, eds., Springer, pp. 183–192.

[16] Uicker, J. J., Ravani, B., and Sheth, P. N., 2013. *Matrix methods in the design analysis of mechanisms and multibody systems*. Cambridge University Press.

[17] Piipponen, S., and Tuomela, J., 2013. "Algebraic analysis of kinematics of multibody systems". *Mechanical Sciences,* ***4***(1), pp. 33–47.

[18] Golubitsky, M., and Guillemin, V., 2012. *Stable Mappings and Their Singularities*. Graduate Texts in Mathematics. Springer, New York.

[19] Gibson, C., and Selig, J., 1988. "Movable hinged spherical quadrilaterals—I". *Mechanism and Machine Theory,* ***23***(1), pp. 13–18.

[20] Gibson, C., and Marsh, D., 1989. "On the linkage varieties of watt 6-bar mechanisms—I. basic geometry". *Mechanism and Machine Theory,* ***24***(2), pp. 105–113.

[21] Grashof, F., 1883. *Theoretische Maschinenlehre*, Vol. 2. Verlag L. Voss, Leipzig.

Appendix A: Determination of Σf for 3RRR PPM

To illustrate the derivation of the conditions in Eqn. 28, eight of the 6×6 minors are shown. In the following, we write $s_{ij} = \sin(\theta_i - \theta_j)$ and similarly for cosine.

$$S_1 = \begin{bmatrix} 1 & 0 & l_1 s_1 & 0 & 0 & l_4 s_4 \\ 0 & 1 & -l_1 c_1 & 0 & 0 & -l_4 c_4 \\ 1 & 0 & 0 & l_2 s_2 & 0 & 0 \\ 0 & 1 & 0 & -l_2 c_2 & 0 & 0 \\ 1 & 0 & 0 & 0 & l_3 s_3 & 0 \\ 0 & 1 & 0 & 0 & -l_3 c_3 & 0 \end{bmatrix}, \quad S_2 = \begin{bmatrix} 1 & 0 & l_1 s_1 & 0 & 0 & 0 \\ 0 & 1 & -l_1 c_1 & 0 & 0 & 0 \\ 1 & 0 & 0 & l_2 s_2 & 0 & l_5 s_5 \\ 0 & 1 & 0 & -l_2 s_2 & 0 & -l_5 c_5 \\ 1 & 0 & 0 & 0 & l_3 s_3 & 0 \\ 0 & 1 & 0 & 0 & -l_3 c_3 & 0 \end{bmatrix},$$

$$S_3 = \begin{bmatrix} 1 & 0 & l_1 s_1 & 0 & 0 & 0 \\ 0 & 1 & -l_1 c_1 & 0 & 0 & 0 \\ 1 & 0 & 0 & l_2 s_2 & 0 & 0 \\ 0 & 1 & 0 & -l_2 c_2 & 0 & 0 \\ 1 & 0 & 0 & 0 & l_3 s_3 & l_6 s_6 \\ 0 & 1 & 0 & 0 & -l_3 c_3 & -l_6 c_6 \end{bmatrix}, \quad S_4 = \begin{bmatrix} 1 & 0 & l_1 s_1 & 0 & 0 & 0 \\ 0 & 1 & -l_1 c_1 & 0 & 0 & 0 \\ 1 & 0 & 0 & l_2 s_2 & 0 & -a_1 s_7 \\ 0 & 1 & 0 & -l_2 c_2 & 0 & a_1 c_7 \\ 1 & 0 & 0 & 0 & l_3 s_3 & -a_2 s_{\alpha 7} \\ 0 & 1 & 0 & 0 & -l_3 c_3 & a_2 c_{\alpha 7} \end{bmatrix},$$

$$S_5 = \begin{bmatrix} 1 & 0 & l_1 s_1 & 0 & l_4 s_4 & 0 \\ 0 & 1 & -l_1 c_1 & 0 & -l_4 c_4 & 0 \\ 1 & 0 & 0 & l_2 s_2 & 0 & l_5 s_5 \\ 0 & 1 & 0 & -l_2 c_2 & 0 & -l_5 c_5 \\ 1 & 0 & 0 & 0 & 0 & 0 \\ 0 & 1 & 0 & 0 & 0 & 0 \end{bmatrix}, \quad S_6 = \begin{bmatrix} 1 & 0 & l_1 s_1 & 0 & l_4 s_4 & 0 \\ 0 & 1 & -l_1 c_1 & 0 & -l_4 c_4 & 0 \\ 1 & 0 & 0 & l_2 s_2 & 0 & 0 \\ 0 & 1 & 0 & -l_2 c_2 & 0 & 0 \\ 1 & 0 & 0 & 0 & 0 & l_6 s_6 \\ 0 & 1 & 0 & 0 & 0 & -l_6 c_6 \end{bmatrix},$$

$$S_7 = \begin{bmatrix} 1 & 0 & l_1 s_1 & 0 & l_4 s_4 & 0 \\ 0 & 1 & -l_1 c_1 & 0 & -l_4 c_4 & 0 \\ 1 & 0 & 0 & l_2 s_2 & 0 & -a_1 s_7 \\ 0 & 1 & 0 & -l_2 c_2 & 0 & a_1 c_7 \\ 1 & 0 & 0 & 0 & 0 & -a_2 s_{\alpha 7} \\ 0 & 1 & 0 & 0 & 0 & a_2 c_{\alpha 7} \end{bmatrix} \quad S_8 = \begin{bmatrix} 1 & 0 & l_1 s_1 & 0 & 0 & 0 \\ 0 & 1 & -l_1 c_1 & 0 & 0 & 0 \\ 1 & 0 & 0 & l_2 s_2 & l_5 s_5 & 0 \\ 0 & 1 & 0 & -l_2 c_2 & -l_5 c_5 & 0 \\ 1 & 0 & 0 & 0 & 0 & l_6 s_6 \\ 0 & 1 & 0 & 0 & 0 & -l_6 c_6 \end{bmatrix}$$

Their determinants, together with the other 76, must vanish simultaneously for a singular point of f:

$$
\begin{aligned}
\det(S_1) &= -(s_{23})(s_{14})l_1l_2l_3l_4, \\
\det(S_2) &= (s_{13})(s_{25})l_1l_2l_3l_5, \\
\det(S_3) &= -(s_{12})(s_{36})l_1l_2l_3l_6, \\
\det(S_4) &= [-a_1(s_{13})(s_{27}) + a_2(s_{12})(s_{\alpha 37})]\, l_1l_2l_3, \\
\det(S_5) &= -(s_{14})(s_{25})l_1l_2l_4l_5, \\
\det(S_6) &= (s_{12})(s_{26})l_1l_2l_4l_6, \\
\det(S_7) &= (s_{14})[a_1(s_{27}) + a_2(s_{\alpha 27})]l_1l_2l_4, \\
\det(S_8) &= -(s_{16})(s_{25})l_1l_2l_5l_6,
\end{aligned} \tag{32}
$$

where $s_{\alpha 37} = \sin(\alpha - \theta_3 + \theta_7)$ and $s_{\alpha 27} = \sin(\alpha - \theta_2 + \theta_7)$. Assume that $l_k \neq 0$, $k = 1, \ldots 6$, then it is clear from Eqn. 32 that:

$$
\begin{aligned}
\det(S_1) &\iff \theta_2 = \theta_3 \mod \pi \text{ or } \theta_1 = \theta_4 \mod \pi \\
\det(S_2) &\iff \theta_1 = \theta_3 \mod \pi \text{ or } \theta_2 = \theta_5 \mod \pi \\
\det(S_3) &\iff \theta_1 = \theta_2 \mod \pi \text{ or } \theta_3 = \theta_6 \mod \pi \\
\det(S_5) &\iff \theta_1 = \theta_4 \mod \pi \text{ or } \theta_2 = \theta_5 \mod \pi \\
\det(S_6) &\iff \theta_1 = \theta_2 \mod \pi \text{ or } \theta_2 = \theta_6 \mod \pi \\
\det(S_8) &\iff \theta_1 = \theta_6 \mod \pi \text{ or } \theta_2 = \theta_5 \mod \pi
\end{aligned}
$$

From these and other similar equations we deduce that one of the sets of equalities in Eqns. 28 must hold. In all such cases, expressions such as those in $\det(S_4)$ and $\det(S_7)$ also vanish, ensuring singularity.

Appendix B: Calculation of 3RRR Grashof-type conditions

Let us consider a configuration where $\theta_1 = \theta_2 = \theta_4 = \theta_5 = \theta_7 \mod \pi$, satisfying singularity set in Eqn. 28a and substitute it into $f(\theta_i, x_i, y_i) = 0$ where f is given in Eqn. 26. It follows that $c_j = \pm c_i, s_j = \pm s_i, i, j = 1, 2, 4, 5, 7$. Eliminating x_i, y_i, $i = 1, \ldots, 7$ from the first 14 equations, we end up with the following relations for the design parameters and pose rotations in Fig 4:

$$\mu c_1 = b_1, \tag{33a}$$

$$\mu s_1 = 0, \tag{33b}$$

$$\xi c_1 = a_2 s_1 s_\alpha + l_3 c_3 + l_6 c_6 + b_2 c_\beta, \tag{33c}$$

$$\xi s_1 = -a_2 c_1 s_\alpha + l_3 s_3 + l_6 s_6 + b_2 s_\beta, \tag{33d}$$

where $\mu = \pm a_1 \pm l_1 \pm l_4 \pm l_2 \pm l_5$ and $\xi = \pm a_2 c\alpha \pm l_1 \pm l_4$. Assuming $b_1 > 0$, Eqns. 33a and 33b imply that $\mu \neq 0$ and $\theta_1 = 0$ or π and thus the generalised Grashof condition $\mu = b_1$ in Eqn. 29 is readily obtained.

At the same time, Eqns. 33c and 33d imply that, in such a singular configuration, θ_3, θ_6 may comprise four potentially different combinations, so the limb $l_3 l_6$ may be positioned in 4 different configurations (either feasible or infeasible) as illustrated Fig. 5a by blue and red dashed lines. Mathematically speaking, we can write Eqns. 33c and 33d as linear equations in c_3, s_3, c_6, s_6 together with the identities $c_3^2 + s_3^2 = 1, c_6^2 + s_6^2 = 1$:

$$l_3 c_3 + l_6 c_6 + b_2 c_\beta - \xi = 0, \tag{34a}$$

$$l_3 s_3 + l_6 s_6 + b_2 s_\beta - a_2 s_\alpha = 0 \tag{34b}$$

This gives four equations in the four variables c_3, s_3, c_6, s_6 and hence can have up to four distinct (complex) solutions. One way to view this is that solving Eqns. 34a and 34b for c_3, s_3 and substituting them into $c_3^2 + s_3^2 = 1$ gives:

$$(\xi - b_2 c_\beta - l_6 c_6)^2 + (a_2 s\alpha - b_2 s_\beta - l_6 s_6)^2 = l_3^2 \tag{35}$$

which represents a circle, intersecting the circle $c_6^2 + s_6^2 = 1$ in at most two real points.

Finally, let us consider a configuration where $\theta_1 = \theta_2 = \theta_3 = \theta_4 = \theta_5 = \theta_6 \mod \pi$, satisfying singularity set in Eqn. 28d and substitute the conditions into Eqn. 26. It follows that $c_j = \pm c_i, s_j = \pm s_i, i, j = 1, 2, 3, 4, 5, 6$. By setting $f = \mathbf{0}$ and eliminating x_i, y_i, $i = 1, \ldots, 7$, we end up with the following four linear relations in c_1, s_1, c_7, s_7:

$$a_1 c_7 - \zeta c_1 = b_1, \tag{36a}$$

$$a_1 s_7 - \zeta s_1 = 0, \tag{36b}$$

$$a_2 c_\alpha c_7 - a_2 s_\alpha s_7 - \vartheta c_1 = b_2 c_\beta, \tag{36c}$$

$$a_2 s_\alpha c_7 + a_2 c_\alpha s_7 - \vartheta s_1 = b_2 s_\beta \tag{36d}$$

where $\zeta = \pm l_1 \pm l_4 \pm l_2 \pm l_5$ and $\vartheta = \pm l_1 \pm l_4 \pm l_3 \pm l_6$. Solving these and combining with the identities $c_1^2 + s_1^2 = c_7^2 + s_7^2 = 1$ gives the Grashof-type conditions Eqn. 31. We conjecture that these equations equate three geometric expressions relating to the three closed-loop chains in Fig. 4, that enable a feasible configuration in which the three limbs are parallel.